

Radiative Penguin decays at Belle

Jin Li (for the Belle Collaboration)
University of Hawaii, Honolulu, HI 96822, USA

We present recent progresses in radiative penguin decays of B meson using a large sample of $B\bar{B}$ pairs recorded at the $\Upsilon(4S)$ resonance with the Belle detector at the KEKB asymmetric energy e^+e^- collider. We report precise measurement of inclusive $b \rightarrow s\gamma$ branching ratio with cut $E_\gamma > 1.7$ GeV, first measurement of time-dependent CP-violation in $B^0 \rightarrow K_s \rho^0 \gamma$, measurement of $B^+ \rightarrow K^+ \eta' \gamma$ branching fraction, and improved branching fraction results for $B^0 \rightarrow (\rho, \omega) \gamma$ with new CP and isospin violation results in the mode.

1. Introduction

Radiative B decay proceeds through a penguin loop diagram in the Standard Model (SM). New particles beyond the SM may contribute in the loop diagrams. In this paper, we present recent Belle results on various radiative B decay topics below. Inclusive $b \rightarrow s\gamma$ measurements will constrain New Physics from the branching fraction as well as determining b -quark mass and motion from photon energy spectrum. Time dependent CP asymmetry in $b \rightarrow s\gamma$ transition can probe for right-handed coupling which is not present in SM. Measurements of exclusive mode $B \rightarrow \eta' K \gamma$ and $B \rightarrow (\rho, \omega) \gamma$ can probe deviations from SM by the branching fraction and CP asymmetry.

In all these studies, large continuum background from $e^+e^- \rightarrow q\bar{q}$ events ($q = u, d, s, c$) has been suppressed using event topology variables. In exclusive modes, two kinematic variable $M_{bc} = \sqrt{E_{\text{beam}}^2 - p_B^{*2}}$ and $\Delta E = E_B^* - E_{\text{beam}}$ are commonly used. Here E_{beam} is the beam energy and E_B^* and p_B^* is the energy and momentum of a B candidate, all defined in the $\Upsilon(4S)$ frame.

2. Inclusive $b \rightarrow s\gamma$ measurement

In this fully inclusive method, $b \rightarrow s\gamma$ decay is studied using a 604.6fb^{-1} ON data sample taken at the $\Upsilon(4S)$ resonance, and 68.3fb^{-1} OFF data sample taken at an energy 60 MeV below the resonance. Hard photon is selected from well isolated ECL clusters with the shower shape consistent with a photon, and required to have a center-of-mass energy $E_\gamma^* > 1.4$ GeV. π^0 and η vetoes are then applied.

First, the photon energy spectrum measured in OFF data is scaled by luminosity to the expected number of non- $B\bar{B}$ events in ON data and subtracted, shown in Fig. 1(a). Here the OFF spectrum has been corrected due to the slight lower energy than ON events. Then the backgrounds coming from non-primary photons from B mesons subtracted from the obtained spectrum. From Monte Carlo (MC) study, six background categories are considered (Fig. 1(b)): (i) photons from $\pi^0 \rightarrow \gamma\gamma$; (ii) photons from $\eta \rightarrow \gamma\gamma$; (iii) other real photons; (iv) ECL clusters not due to single photons (mainly K_L^0 's and \bar{n} 's); (v) Electrons misidentified as photons; and (vi) beam background. For each of the background category, the shape and yield is corrected from MC using data by selecting them. Then, for each selection criterion used in this analysis, the data-MC efficiency ratio is obtained using appropriate control samples, and is then used to scale the MC background sample. For example, the π^0 veto efficiency is studied using $D^{*+} \rightarrow D^0(K^-\pi^+\pi^0)\pi^+$ decays where only one γ from π^0 is reconstructed.

The raw spectrum shown in Fig. 1(c) is obtained after subtracting the six background categories after scaling. The raw spectrum is then corrected by three step procedure: (i) divide by the efficiency of the selection; (ii) perform an unfolding which removes the distortion by caused ECL; (iii) divide by efficiency of detection. Then, two additional corrections are applied: (i) to remove cabibbo suppressed $B \rightarrow X_d \gamma$ decays, using the ratio of branching fractions; (ii) to correct the measurements to B -meson rest frame from $\Upsilon(4S)$ frame (boost correction). The partial branching fraction, first moment (mean) and second central moment (variance) of the photon energy spectrum from B decay are obtained as: [1] $\mathcal{B}(B \rightarrow X_s \gamma) = (3.31 \pm 0.19 \pm 0.37 \pm 0.01) \times 10^{-4}$; $\langle E_\gamma \rangle = 2.281 \pm 0.032 \pm 0.053 \pm 0.002$ GeV;

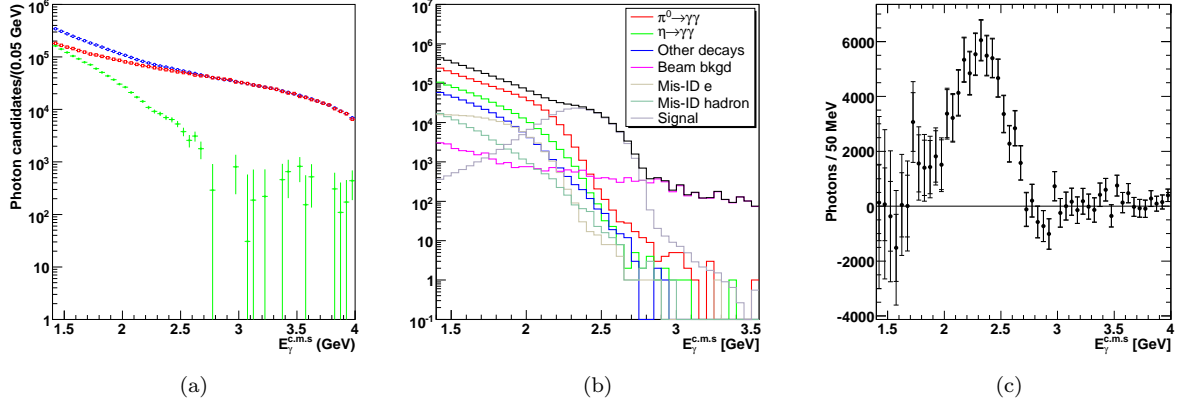


Figure 1: (a) ON data (open circle), scaled OFF data (open square) and continuum background subtracted (filled circle) photon energy spectra of candidates in the c.m.s frame. (b) The spectra of photons from B -meson decays passing selection criteria as predicted using a MC sample. (c) The extracted photon energy spectrum of $B \rightarrow X_{s,d}\gamma$. The two error bars show the statistical and total errors.

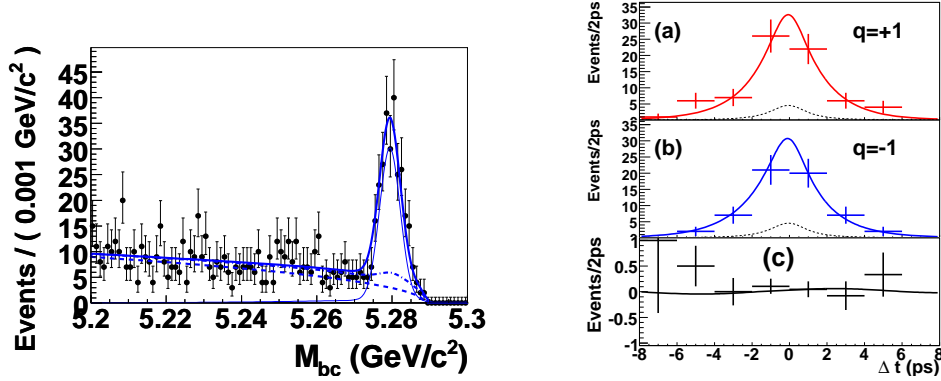


Figure 2: (Left) M_{bc} distributions for $B^0 \rightarrow K_S^0 \pi^+ \pi^- \gamma$ events in ρ^0 region. The dashed and dash-dotted curves are the $q\bar{q}$ and all BG. The thin curve is the total signal and the thick curve is the total PDF. (Right) Fit projections on the Δt distributions for events good-tagged as (a) B^0 and (b) \bar{B}^0 . The raw asymmetry as a function of Δt is shown in (c).

$\langle E_\gamma^2 \rangle - \langle E_\gamma \rangle^2 = 0.0396 \pm 0.0156 \pm 0.0214 \pm 0.0012 \text{ GeV}^2$, where the errors are statistical, systematic and from the boost correction, respectively.

3. Time-dependent CP Asymmetries in $B^0 \rightarrow K_S^0 \rho^0 \gamma$ Decay

In this mode, signal B^0 decay vertex can be reconstructed from two charged pions to calculate the decay time difference Δt between signal and tag side B , thus avoiding K_S^0 vertexing. The $B^0 \rightarrow K_S^0 \rho^0 \gamma$ candidates are selected from the $K_S^0 \pi^+ \pi^- \gamma$ sample by requiring the $\pi^+ \pi^-$ invariant mass to lie in the ρ^0 region, $0.6 \text{ GeV}/c^2 < m_{\pi\pi} < 0.9 \text{ GeV}/c^2$. We first measure the effective CP -violating parameters, \mathcal{S}_{eff} and \mathcal{A}_{eff} , using the final sample and then convert them to the CP -violating parameters of $B^0 \rightarrow K_S^0 \rho^0 \gamma$ using a dilution factor \mathcal{D} .

Fig. 2(left) shows a fit to M_{bc} in ΔE signal region after vertexing. We obtain 212 ± 17 total signal yield from the total 299 events in the signal M_{bc} region. The \mathcal{S}_{eff} and \mathcal{A}_{eff} parameters are then extracted from an unbinned maximum likelihood fit to the Δt distribution, as $\mathcal{S}_{\text{eff}} = 0.09 \pm 0.27(\text{stat.})^{+0.04}_{-0.07}(\text{syst.})$ and $\mathcal{A}_{\text{eff}} = 0.05 \pm 0.18(\text{stat.}) \pm 0.06(\text{syst.})$. The Δt projection for the fit is shown in Fig. 2(right).

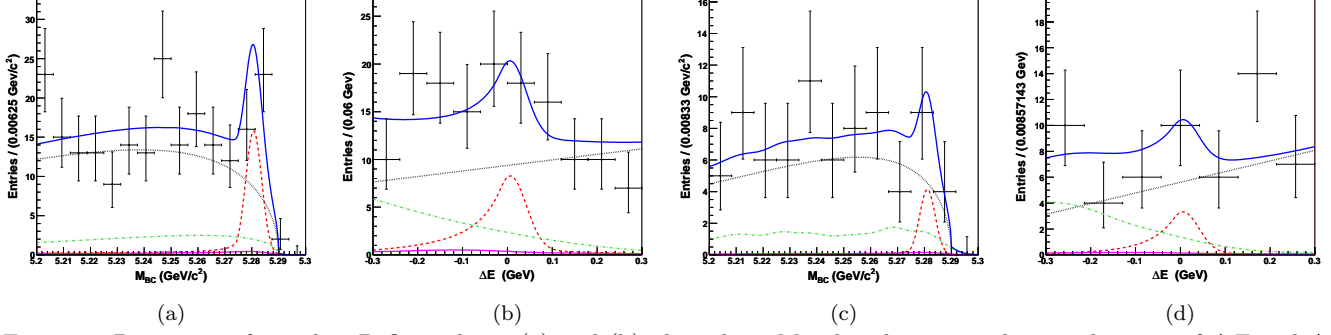


Figure 3: Projections from the 2D fit to data. (a) and (b) plots show M_{bc} distribution in the signal region of ΔE and ΔE distribution in the signal region of M_{bc} , for the $B^+ \rightarrow K^+\eta'\gamma$ mode. The $K\eta'\gamma$ function is shown in dashed red, $q\bar{q}$ in dotted black, $b \rightarrow c$ in dash-dotted green, $b \rightarrow u, d, s$ in solid magenta, and the combined function in solid blue. (c) and (d) are the same for $B^0 \rightarrow K_S^0\eta'\gamma$ mode.

Mode	Yield(events)	ε	\prod	BF(10^{-6})	$S'(\sigma)$	UL(10^{-6})
$B^+ \rightarrow K^+\eta'\gamma$	$32.6^{+11.8}_{-10.8}$	0.027	0.571	$3.2^{+1.2+0.3}_{-1.1-0.3}$	3.3	-
$B^0 \rightarrow K^0\eta'\gamma$	$5.1^{+5.0}_{-4.0}$	0.016	0.197	$2.4^{+2.4+0.4}_{-1.9-0.5}$	1.3	6.3

Table I: The yields, efficiencies(ε), daughter BF's (\prod), measured BF's, fit significances including systematics (S') and upper limits (UL) for the measured decays.

The parameter \mathcal{S}_{eff} is related to \mathcal{S} for $K_S^0\rho^0\gamma$ with a dilution factor \mathcal{D} :

$$\mathcal{D} = \frac{\mathcal{S}_{\text{eff}}}{\mathcal{S}_{K_S^0\rho^0\gamma}} = \frac{\int [|F_A|^2 + 2\Re(F_A^*F_B) + F_B^*(\bar{K})F_B(K)]}{\int [|F_A|^2 + 2\Re(F_A^*F_B) + |F_B|^2]},$$

where F_A, F_B are photon-helicity averaged amplitudes for $B^0 \rightarrow K_S^0\rho^0(\pi^+\pi^-)\gamma$ and $B^0 \rightarrow K^{*\pm}(K_S^0\pi^\pm)\pi^\mp\gamma$, respectively. From the study to $(K^+\pi^-\pi^+)$ system in charged mode $B^+ \rightarrow K^+\pi^-\pi^+\gamma$ using isospin symmetry, we obtain $\mathcal{D} = 0.83^{+0.19}_{-0.03}$. In summary, we measure the CP -violating parameter $\mathcal{S}_{K_S^0\rho^0\gamma} = 0.11 \pm 0.33(\text{stat.})^{+0.05}_{-0.09}(\text{syst.})$ [2]. This agrees with SM prediction $\mathcal{S}_{K_S^0\rho^0\gamma} \approx 0.03$ [3].

4. Evidence for $B \rightarrow \eta'K\gamma$ Decays at Belle

The exclusive mode $B \rightarrow \eta'K\gamma$ is analyzed using 604.6fb^{-1} of data, for both charged and neutral mode. η' mesons are reconstructed as $\eta' \rightarrow \eta\pi^+\pi^-$ and $\eta' \rightarrow \rho^0\gamma$. η mesons are reconstructed as $\eta \rightarrow \gamma\gamma$ and $\eta \rightarrow \pi^+\pi^-\pi^0$. D^0 mass veto on $m_{K^+\pi^-}$ for any charged pion in the event and J/ψ mass veto on $m_{\eta'\gamma}$ are applied to suppress $b \rightarrow c$ events.

The signal yield is extracted by fitting 2D M_{bc} and ΔE distributions shown in Fig. 3. All final states are combined in to one distribution for fitting for the charged mode, so does the neutral mode. The signal shape is calibrated using large samples of $B \rightarrow K^*(892)\gamma$ data and MC. The continuum parameters are floated in the fit. Table I shows the fit results and branching fractions (BFs). The efficiencies are weighted by background-subtracted $M(K\eta')$ data distribution. Systematic errors are included in the likelihood by convolving the likelihood functions to calculate the significances and upper limits.

5. $b \rightarrow d\gamma$ update by Belle

Belle updated the measurements of $B \rightarrow \rho\gamma$, $B \rightarrow \omega\gamma$ decays using a sample of 657 million B mesons. Three signal modes, $B^+ \rightarrow \rho^+\gamma$, $B^0 \rightarrow \rho^0\gamma$ and $B^0 \rightarrow \omega\gamma$ are reconstructed with subdecay modes $\rho^+ \rightarrow \pi^+\pi^0$, $\rho^0 \rightarrow \pi^+\pi^-$, $\omega \rightarrow \pi^+\pi^-\pi^0$. A helicity selection of the ρ and ω is applied to suppress decays with π^0/η from B .

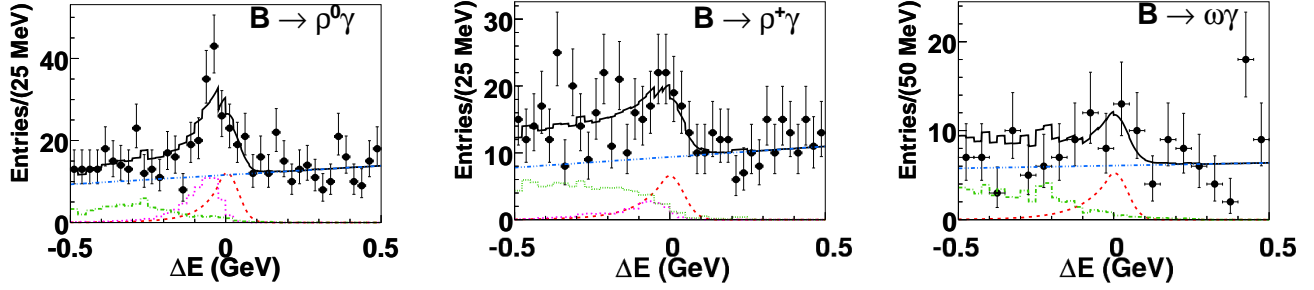


Figure 4: Projections of the fit results to ΔE in M_{bc} signal region for $B^+ \rightarrow \rho^0\gamma$, $B^0 \rightarrow \rho^+\gamma$ and $B^0 \rightarrow \omega\gamma$. Curves show the signal (dashed, red), continuum (dot-dot-dashed, blue), $B \rightarrow K^*\gamma$ (dotted, magenta), other backgrounds (dash-dotted, green), and the total fit result (solid).

Table II: Yield, significance with systematic uncertainty, efficiency, and branching fraction (\mathcal{B}) for each mode. The first and second errors in the yield and \mathcal{B} are statistical and systematic, respectively. The sub-decay $\mathcal{B}(\omega \rightarrow \pi^+\pi^-\pi^0)$ is included for the $\omega\gamma$ mode.

Mode	Yield	Significance	Efficiency (%)	\mathcal{B} (10^{-7})
$B^+ \rightarrow \rho^+\gamma$	$45.8^{+15.2+2.6}_{-14.5-3.9}$	3.3	8.03 ± 0.59	$8.7^{+2.9+0.9}_{-2.7-1.1}$
$B^0 \rightarrow \rho^0\gamma$	$75.7^{+16.8+5.1}_{-16.0-6.1}$	5.0	14.81 ± 0.95	$7.8^{+1.7+0.9}_{-1.6-1.0}$
$B^0 \rightarrow \omega\gamma$	$17.5^{+8.2+1.1}_{-7.4-1.0}$	2.6	6.58 ± 0.76	$4.0^{+1.9}_{-1.7} \pm 1.3$

A fit to M_{bc} and ΔE (and $M_{K\pi}$ for the $\rho^0\gamma$ mode) for candidates satisfying $|\Delta E| < 0.5$ GeV and $M_{bc} > 5.2$ GeV/ c^2 is performed individually for the three $\rho\gamma/\omega\gamma$ signal modes and the two control modes $K^+\gamma$ and $K^0\gamma$. Significant $K^{*0}\gamma$, $K^{*+}\gamma$ background in the $\rho^0\gamma$ and $\rho^+\gamma$ samples are shifted in ΔE from signal peak. The shift offset of this background is determined from K^* enriched sample from data, which is also used to determine the size using known kaon to pion misidentification rate. The ΔE projections of fit results are shown in Fig. 4. Table II lists the obtained yields and branching fractions [4].

The branching fractions are combined to a single branching fraction $\mathcal{B}(B \rightarrow (\rho, \omega)\gamma) \equiv \mathcal{B}(B^+ \rightarrow \rho^+\gamma) \equiv 2 \times \frac{\tau_{B^+}}{\tau_{B^0}} \mathcal{B}(B^0 \rightarrow \rho^0\gamma) = 2 \times \frac{\tau_{B^+}}{\tau_{B^0}} \mathcal{B}(B^0 \rightarrow \omega\gamma)$, and the ratio to corresponding mode $B \rightarrow K^*\gamma$ is calculated as $\frac{\mathcal{B}(B \rightarrow (\rho, \omega)\gamma)}{\mathcal{B}(B \rightarrow K^*\gamma)} = 0.0284 \pm 0.0050^{+0.0027}_{-0.0029}$. This result is used to relate the ratio of CKM matrix element: $|V_{td}/V_{ts}| = 0.195^{+0.020}_{-0.019}(\text{exp.}) \pm 0.015(\text{th.})$. The isospin asymmetry $A_I(B \rightarrow \rho\gamma) = 2 \frac{\tau_{B^+}}{\tau_{B^0}} \mathcal{B}(B^0 \rightarrow \rho^0\gamma) / \mathcal{B}(B^+ \rightarrow \rho^+\gamma) - 1$ is calculated to be $A_I(B \rightarrow \rho\gamma) = 0.92^{+0.76+0.30}_{-0.71-0.35}$, which agrees with BaBar [5] (note the different definition). The direct CP -violating asymmetry is also measured for the first time by fitting $B^+ \rightarrow \rho^+\gamma$ and $B^- \rightarrow \rho^-\gamma$ events simultaneously, as $A_{CP}(B^+ \rightarrow \rho^+\gamma) = [N(\rho^-\gamma) - N(\rho^+\gamma)] / [N(\rho^-\gamma) + N(\rho^+\gamma)] = -0.11 \pm 0.32 \pm 0.09$.

References

- [1] K. Abe *et al.* [Belle Collaboration], arXiv:0804.1580 [hep-ex].
- [2] J. Li *et al.* [Belle Collaboration], arXiv:0806.1980 [hep-ex].
- [3] D. Atwood, T. Gershon, M. Hazumi and A. Soni, Phys. Rev. D **71**, 076003 (2005) [arXiv:hep-ph/0410036].
- [4] N. Taniguchi *et al.* [Belle Collaboration], Phys. Rev. Lett. **111**, 111801 (2008) [arXiv:0804.4770 [hep-ex]].
- [5] B. Aubert *et al.* [BABAR Collaboration], arXiv:0808.1379 [hep-ex].